Adsorption (2013) 19:1109–1116
DOI 10.1007/s10450-013-9539-y

Adsorption of SO_2 and chlorobenzene on activated carbon

Yangyang Guo · Yuran Li · Tingyu Zhu · Meng Ye · Xue Wang

Received: 5 December 2012 / Accepted: 5 March 2013 / Published online: 15 March 2013

Abstract Activated carbon is very effective for simultaneous removal of multiple pollutants. The adsorption of SO_2 and chlorobenzene modeling of VOCs on activated carbon was investigated in a fixed-bed reactor by four kinds of activated carbon. The results show that the SO_2 adsorption is affected by the BET surface and basic functional groups as C=O and π–π* groups of the carbon, while the chlorobenzene adsorption is strongly affected by the carbon pore structure, with the micropore volume deciding the adsorption amount and larger pores increasing the adsorption rate. The chlorobenzene adsorption is little affected by the chemical properties of activated carbon as the O/C ratio detected by XPS. The effect of SO_2 on the chlorobenzene adsorption was investigated, with the results showing the SO_2 seriously restricts the individual chlorobenzene adsorption and this effect becomes smaller in the presence of O_2. The adsorption products were analyzed by TPD-MS and the initial decomposition temperatures are 380 K for chlorobenzene and 500 K for SO_2, showing that SO_2 is much more stable adsorbed than chlorobenzene. The changes of the carbon functional groups that the CO_2 desorption peak emerges at 700 K and decreases at 1000 K with the chlorobenzene adsorption, were observed by TPD-MS, indicating that the lactone and quinone groups on the carbon are likely to combine with the chlorobenzene and form weakly chemisorbed chlorobenzene.

Keywords Activated carbon · VOCs · Chlorobenzene · SO_2 · Co-adsorption

Y. Guo · Y. Li · T. Zhu (✉) · M. Ye · X. Wang
Research Center for Process Pollution Control, National Engineering Laboratory for Hydrometallurgical Cleaner Production Technology, Institute of Process Engineering, Chinese Academy of Sciences, Beijing 100190, China
e-mail: tyzhu@mail.ipe.ac.cn

Y. Guo
Graduate University of Chinese Academy of Sciences, Beijing 100049, China
e-mail: yyguo@home.ipe.ac.cn

1 Introduction

Industrial flue gases contain not only conventional inorganic pollutants like SO_2, but also volatile organic compounds (VOCs) such as alkane and chlorinated compounds, which can damage human nervous systems and cause cancer. Common treatment processes, such as lime addition or selective catalytic reactions, can remove one acidic gas. Activated carbon adsorption is considered to be the most effective process for simultaneous removal of various pollutants (Agranovski et al. 2005). The activated carbon provides effective oxidation and removal of SO_2 (Liu 2008; Zhang et al. 2007), and is used for effective control of organic pollutants (Vanosdell et al. 1996; Gironi and Piemonte 2011). Activated carbon, with very large surface areas and pore volumes, has hydrophobic graphene layer surfaces and hydrophilic functional groups located on the edges of the graphene layers. Gas adsorption on activated carbon is influenced by both the pore structure and the surface chemistry.

Previous studies of SO_2 adsorption (López et al. 2008; Raymundo-Piñero et al. 2001) in the presence of oxygen and water show that SO_2 is not only physically adsorbed but also chemisorbed. The SO_2 adsorption has been concluded with the carbon micropore structure to show that the optimal pore size for the oxidation of SO_2–SO_3 is around 0.7 nm (Raymundo-Piñero et al. 2000). Izquierdo et al. (2003) demonstrated that the optimal number of oxygen-

functional groups on the carbon would allow fast removal of SO_2.

The predominant properties affecting VOCs adsorption are the micropore volume and the specific surface area of the activated carbon. The surface functional groups have a relatively small effect on adsorption, for example, phenolic groups are slightly helpful to VOCs adsorption (Chiang et al. 2001); however, the surface functional groups can be important if they simultaneously interact with more than two types of molecules. Ghimbeu et al. (2011) showed that ethanol can lead to strong interactions with the carbon surface when cyclohexane is adsorbed preferentially, with the co-adsorption causing more stable ethanol adsorption as demonstrated by the temperature programmed desorption coupled with mass spectroscopy (TPD-MS) method. Mastral et al. (2002) found the coexistence of CO_2 significantly lowered the adsorption capacity of phenanthrene due to the physical competitive effect of both molecules to access the adsorption sites. While the co-adsorption of butane and NO_2 or SO_2 on activated carbon reduces the adsorption capacity for oxide components, but the adsorption of butane is not influenced by SO_2 or NO_2 (Ahnert and Heschel 2002).

Thus, co-adsorption can limit the adsorption amount for certain components. The competitive adsorption and desorption behavior differs due to the different properties of absorbed gases. The SO_2 and chlorobenzene adsorption are studied here on four kinds of activated carbons to investigate the effects of the physic-chemical characteristics of carbon on each component adsorption. The co-adsorption of SO_2 and chlorobenzene are studied with the adsorption products desorbed using TPD-MS to analyze the adsorption process.

2 Experimental

2.1 Materials and characterization

Four commercial activated carbon (AC) samples were selected based on different raw materials (coconut, coal, shell and wood) named AC-N, AC-C, AC-S and AC-W. The samples were dried at 120 °C for 12 h before the experiments, with the properties listed in Table 1. N_2 adsorption was performed at 77 K in an automatic surface area and porosity analyzer (Autosorb iQ, Quantachrome). The surface area (S_{BET}) was calculated from the N_2 adsorption isotherms using the BET equation. The total pore volume (V_T) was accessed from the amount of N_2 adsorbed at $p/p_0 = 0.95$. The micropore volume (V_{mi}) was calculated using the Horvath–Kawazoe (HK) equation and the Dubinin–Radushkevich (DR) equation with the average micropore width (D_0) was obtained by the DR equation.

Table 1 Characterization of the various activated carbons

Sample	AC-N	AC-C	AC-S	AC-W
S_{BET} (m^2/g)	980.7	892.9	882.1	460.9
V_T (ml/g)	0.480	0.418	0.401	0.332
$V_{mi\text{-}HK}$ (ml/g)	0.390	0.357	0.351	0.189
$V_{mi\text{-}DR}$ (ml/g)	0.385	0.356	0.361	0.184
D_0 (nm)	1.449	1.725	0.715	1.523
O/C (%)	20.65	21.85	14.94	16.91
Basic groups (mmol/g)	0.165	0.207	0.080	0.083

The surface chemical state and the O/C atomic ratio of the samples were measured using X-ray photoelectron spectroscopy (XPS, ESCALab 250, Thermo Electron) with an Al Kα X-ray source (1486.6 eV) at a constant recording ratio of 40. The X-ray source was run at a reduced power of 150 W. The pressure in the analysis chamber was maintained at 10^{-8} Torr or lower during each measurement. To compensate for surface charge effects, all binding energies were referenced to the C1s hydrocarbon peak at 284.6 eV. Benzoic acid titration was used to quantitatively measure the basic functional groups. 0.50 g of each sample was placed in a vial with 50 ml of 0.01 mol/L Benzoic acid solution, sealed and shaken for 24 h at 20 °C, and then filtrated. 20 ml of the filtrate was titrated with 0.01 mol/L NaOH. The number of basic sites was calculated from the amount of benzoic acid that reacted with the carbon with the results given in Table 1.

2.2 SO_2 and chlorobenzene adsorption and desorption tests

The adsorption of SO_2 and chlorobenzene on the activated carbons was investigated in a fixed-bed reactor. The quartz tube reactor was 20 mm in diameter and 500 mm in height with a sieve plate in the middle. 0.50 g of each sample with particle sizes of 38–62 μm was loaded on the plate for each experiment. The reaction temperature was 120 °C. The gas flow rate at standard state was 300 ml/min. The simulated flue gas consisted of SO_2, chlorobenzene vapor, O_2 and a balance of N_2. The chlorobenzene vapor was generated using N_2 from a bubbling container bathed in 40 °C water. After mixing in the mixing vessel, the gas was fed into the reactor with the effluent gas continuously detected by a quadruple mass spectrometer (GAM200, IPI). Before each test, the mass spectrometer was purged with high purity nitrogen for 4 h. The gases detected by the mass spectrometer were identified by using the major mass ion 64 for SO_2, 112 for chlorobenzene, 44 for CO_2 and 32 for O_2. The chlorobenzene concentration was calibrated using gas chromatography (7890, Agilent) at 200 ± 10 ppm (volume concentration), the SO_2 concentration was controlled by a

mass flow controller that gave 1000 ppm and the O_2 concentration was 5 vol.%.

The SO_2 and chlorobenzene adsorption amounts of the activated carbon were determined by numerical integration of the experimental data, with the amount of adsorbate adsorbed by the adsorbent calculated as:

$$v = \frac{F_0 M}{22.4 \times m_0} \int_0^t (C_0 - C_t)\, dt \quad (1)$$

where v is the adsorbent adsorption amount, F_0 is the volumetric feed flow rate, M is the mole fraction of the adsorbate in the feed, m_0 is the adsorbent mass used inside the bed, C_0 is the adsorbate feed concentration, and C_t is the adsorbate concentration at time, t.

Temperature programmed desorption coupled with mass spectroscopy (TPD-MS) was used to investigate the adsorption products and the specific interactions between the carbon materials and the adsorbate during the adsorption. The heating rate was set at 10 °C/min and the desorption was measured in the range of 30–900 °C. The effluent gases CO_2, chlorobenzene, SO_2 and CO were monitored continuously by the mass spectroscopy, with CO identified by the major mass ion 12 and the CO signal obtained by deduction of the CO_2 from the total C.

3 Results and discussion

3.1 SO_2 adsorption

The effect of the activated carbon properties on the SO_2 adsorption was investigated by measuring the SO_2 adsorption on the four samples with the results shown in Fig. 1. The line shapes are similar, with the amount of SO_2 adsorbed quickly increasing initially, then increasing slowly over time. The SO_2 adsorption amount still increases at 180 min, which indicates that the SO_2 adsorption has not yet reached saturation.

The empirical Bangham equation, shown in Eq. (2) (Bangham and Burt 1924), for SO_2 adsorption fits this experimental data very well as shown in Fig. 1.

$$v = kt^{1/m} \quad (2)$$

where ν is the adsorption amount, k is the adsorption rate constant and m is the constant. R^2 is the correlation coefficient. Table 2 shows the Bangham parameters and SO_2 adsorption amounts, with AC-C having the largest adsorption amount and adsorption rate for SO_2. The rate is less for AC-N following AC-S and AC-W. SO_2 adsorption can be affected by the carbon structure, with the SO_2 adsorption amount increasing with the BET surface increases.

Although AC-N has the largest BET surface and micropore volume as shown in Table 1, its SO_2 adsorption

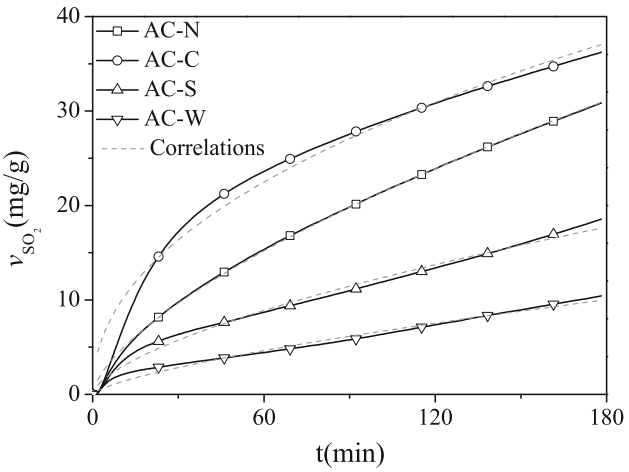

Fig. 1 SO_2 adsorption curves and the Bangham correlations (Adsorption conditions: 1000 ppm SO_2, 5 % O_2, N_2, 120 °C)

Table 2 SO_2 adsorption amount and Bangham correlation results

Sample	k	m	SO_2 amount (mg/g)[a]	R^2
AC-N	1.052	1.533	30.85	0.9989
AC-C	3.436	2.179	36.22	0.9779
AC-S	0.675	1.589	18.56	0.9900
AC-W	0.261	1.423	10.43	0.9837

[a] SO_2 adsorption amounts were calculated based on Eq. (1)

is less than for AC-C, which indicates that the SO_2 adsorption is not only determined by the carbon structure, but also by the chemical properties of the carbon. The character of the activated carbon surfaces is closely related to the surface oxygen functional groups, which can be classified into acidic, basic, neutral classes (Shafeeyan et al. 2010). Functional groups such as carboxyl acid, lactone and phenolic hydroxyl have been postulated as the sources of the surface acidity. Chromene, ketone and pyrone can contribute to the carbon basicity, and the resonating π-electrons of carbon aromatic rings can act as Lewis bases (Montes-Morán et al. 2004). The oxygen functional groups measured by XPS, can be identified by examining the C1s and O1s core regions, with the results shown in Fig. 2. The main C1s peak was divided into five peaks based on the binding energies of 284.6, 286, 287.3, 288.6, 290.4 eV corresponding to the C–C, C–O, C=O, COOH and π–π* groups (Goworek et al. 1997), O1s peak was divided into three peaks based on the binding energies of 531.1, 533.2, 535.2 eV corresponding to the C–O, C=O groups and chemisorbed O (Biniak et al. 1997).

The area percentages of the peaks reflect the relative content of each group. The results in Fig. 2b show that AC-C and AC-W have more C=O and π–π* groups, while AC-N and AC-S have more C–O and COOH groups. The

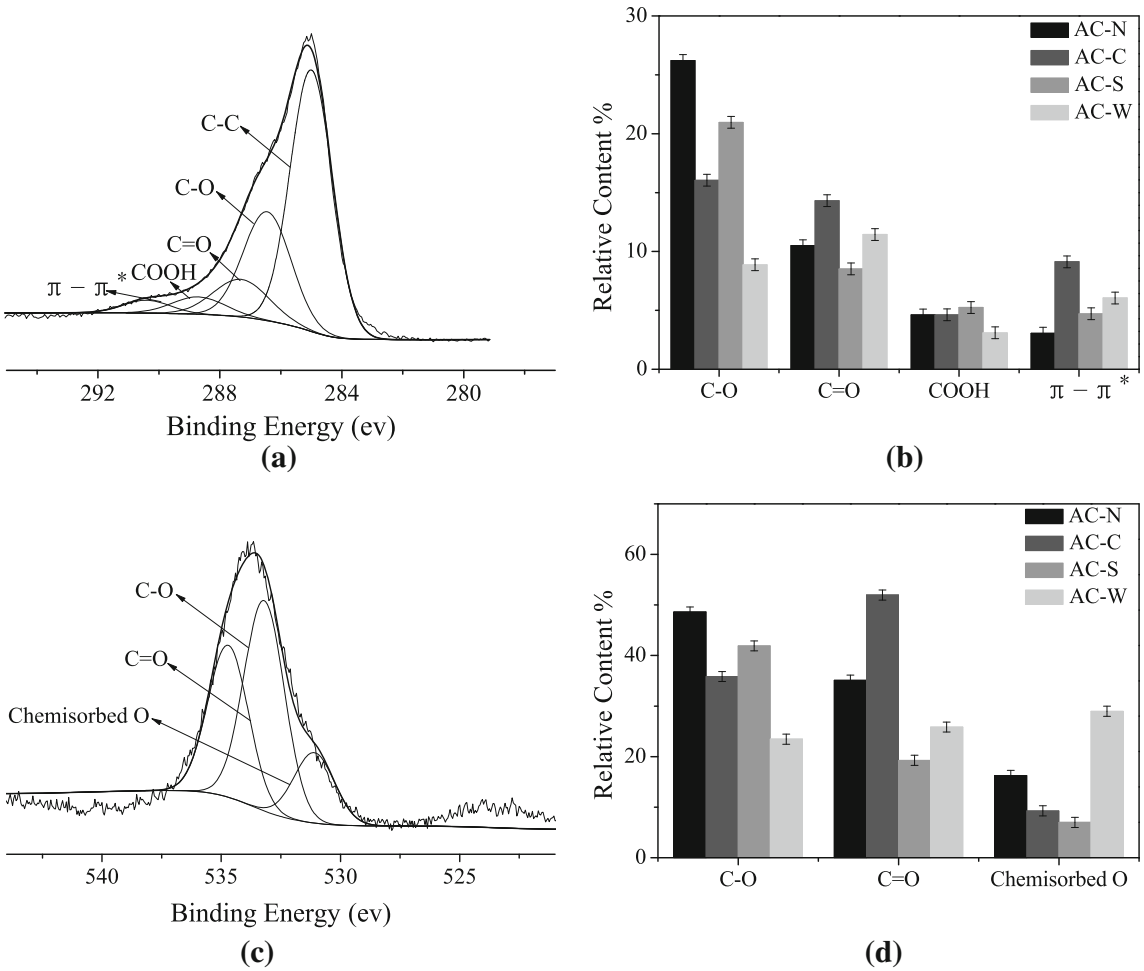

Fig. 2 Oxygen functional groups **a** C1s spectrum of the oxygen functional groups on AC-N, **b** Area percentages of the functional groups on all samples, **c** O1s spectrum of the oxygen functional groups on AC-N, **d** Area percentages of the functional groups on all samples

results of C–O and C=O from O1s level in Fig. 2d are consistency with that in Fig. 2b. Classifications of the functional groups give C–O and COOH groups as acidic and C=O and π–π* groups as basic. Moreover, as shown in Table 1, the O/C ratio for AC-C is 21.85 % and the basic group content is 0.207 mmol/g, both of which are the highest among the four samples. Thus, the basic functional groups benefit for acidic gas chemical adsorption, which is similar with the result obtained by Karatepe et al. (2008). The experimental results also indicate that the SO_2 adsorption is not only determined by the carbon BET surface, but also by the chemical properties, especially the basic functional groups as C=O and π–π* groups of the carbon.

3.2 Chlorobenzene adsorption

The effect of the activated carbon properties on the chlorobenzene adsorption was found by measuring the cumulative chlorobenzene adsorption on the four samples with the results shown in Fig. 3. The amount of chlorobenzene adsorbed increased linearly with time in the first 2 h, and then tended to flatten to saturation, which differs from the SO_2 adsorption.

The Langmuir equation, shown in Eq. (3), need to correlate the data since it is commonly used for the absorption of organic gases on porous materials (Fournel et al. 2010).

$$v/v_e = 1 - e^{-\varphi t} \tag{3}$$

where ν is the adsorption amount, mg/g, and ν_e is the saturated adsorption amount, mg/g, φ is the summation of the adsorption rate constant and the desorption rate constant. The correlation results are shown in Fig. 3 and Table 3.

The chlorobenzene adsorption amounts are highest for AC-N and lower for AC-S then AC-C and AC-W. The adsorption amounts of the four carbons positively correlate to the total pore volume with $R^2 = 0.938$, which indicates that chlorobenzene adsorption is strongly affected by the carbon pore structure. The chlorobenzene adsorption has

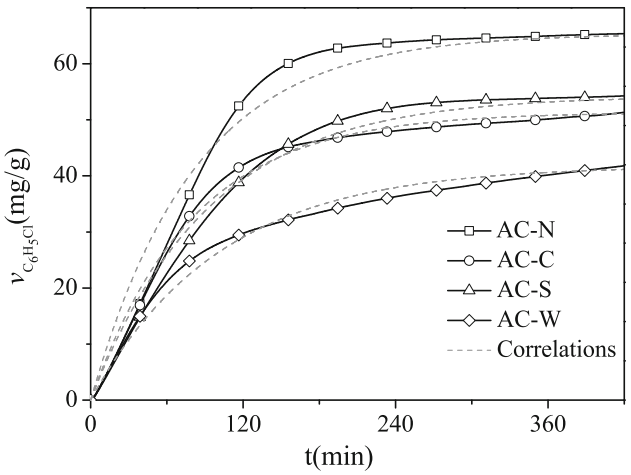

Fig. 3 Chlorobenzene adsorption and the Langmuir correlations (adsorption conditions: 200 ± 10 ppm chlorobenzene, 5 % O_2, N_2, 120 °C)

Table 3 C_6H_6Cl adsorption amount and Langmuir correlation results

Sample	φ	C_6H_6Cl amount (mg/g)[a]	R^2
AC-N	0.0122	65.17	0.9678
AC-C	0.0125	51.26	0.9893
AC-S	0.0108	54.08	0.9846
AC-W	0.0099	41.79	0.9826

[a] The chlorobenzene adsorption amounts were calculated based on Eq. (1)

little relationship with carbon chemical properties with a correlation coefficient of only 0.136 between the chlorobenzene adsorption amount and the O/C ratio.

The QSDFT (Quenched solid density functional theory) split model was used to analyze the pore size distribution with the results shown in Fig. 4. The pore structures of these samples are mainly micropores with the majority of the pore sizes between 0.8 nm and 1.1 nm and mesoporous pore is distributed around 3.4 nm. AC-N and AC-C have a continuously pore size distribution between 1.1 and 2.4 nm, while the pore sizes in AC-S are mainly 0.60, 0.79 and 1.10 nm with the smallest average pore diameter among the samples.

When the pore size is near the molecular diameter, the adsorption process becomes much more easily (Karpowicz et al. 2000). The AC-S pore sizes are around 0.8 nm as the closest with the diameter of the chlorobenzene molecule 0.77 nm (Asnin et al. 2008), with the chlorobenzene adsorption amount of AC-S being 54.08 mg/g and 5.5 % larger than that of AC-C. Larger pores provide access for the adsorbed gas to enter the micropores to allow multilayer adsorption that increases the adsorption (Mastral et al. 2002). φ of 0.0122 for AC-N and 0.0125 for AC-C are larger

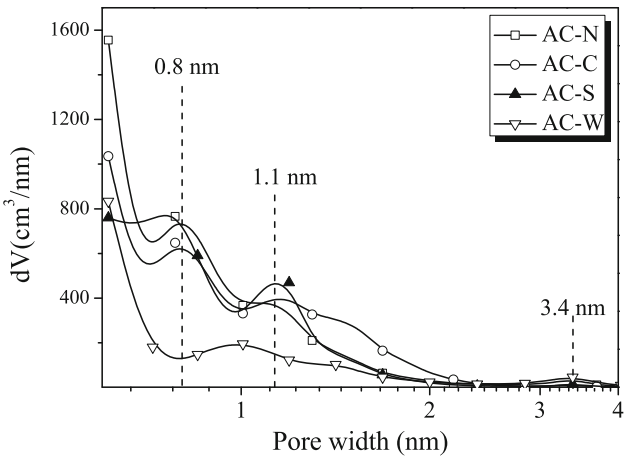

Fig. 4 Sample pore size distributions

due to the wider pores; while, φ of 0.0108 for AC-N is smaller due to the narrow pore size. AC-W has the widest pore size with φ of 0.0099 which is the lowest. Since φ is the summation of the adsorption and desorption constants, desorption on AC-W is much quicker due to its widest pores.

Generally, higher boiling point gases are more easily to be adsorbed. The boiling point of chlorobenzene is 131.7 and −10 °C for SO_2, so the adsorption amount for chlorobenzene is larger than for SO_2 on the same carbon, with 65.17 mg/g chlorobenzene and 30.85 mg/g SO_2 adsorbed on AC-N. Unlike the SO_2 adsorption, the chlorobenzene adsorption is mainly affected by the physical structure of the carbon. The micropore volume then determines the adsorption amount, with large size pores needed to increase the adsorption rate.

3.3 Simultaneous adsorption of SO_2 and chlorobenzene

The activated carbon properties affect the adsorption amount for single component gases. However, the influence of gas mixtures on each other need to be further investigated on the same carbon. The AC-N carbon sample was used to study the competitive adsorption of binary gases on carbon.

As shown in Fig. 5, the breakthrough times and the slopes of the curves indicate the impacts of SO_2 and O_2 on the chlorobenzene adsorption. Several theoretical models have been proposed in the literature to simulate breakthrough curves (Suzuki 1990). The Yoon and Nelson model (Huang et al. 1999) is used here due to its simplicity and capacity to satisfactorily fit the experimental breakthrough curves, and is expressed as

$$t = \tau + \frac{1}{k'} \ln \frac{C_b}{C_i - C_b} \quad (4)$$

where t is the breakthrough time, τ is the time required for 50 % adsorbate breakthrough, k' is the rate constant, C_b

and C_i are the breakthrough effluent and inlet concentrations. Figure 5 shows the experimental and theoretical breakthrough curves for four cases, with the correlation parameters listed in Table 4.

As shown by all the correlation coefficients being over 0.98 in Table 4, the Yoon and Nelson model is appropriate for predicting the breakthrough time. The parameter τ positively correlates to the chlorobenzene adsorption amount with $R^2 = 0.979$. As mentioned in Sect. 3.2, the microporosity volume determines the adsorption amount, so τ depends on the adsorbent microporosity. The addition of other gases into the chlorobenzene atmosphere increases the rate constant k', which means that the adsorption rate for chlorobenzene alone is the lowest among the four cases.

The presence of O_2 increases the chlorobenzene adsorption by only 0.84 %, which means that the promotion effect of O_2 can be ignored. Santoro et al. (Santoro et al. 2003) pointed out that oxidation of organic gases can be catalyzed by some oxygen complexes (C–O), such as can formed on the carbon surface in the presence of O_2, but the oxidation is relatively small.

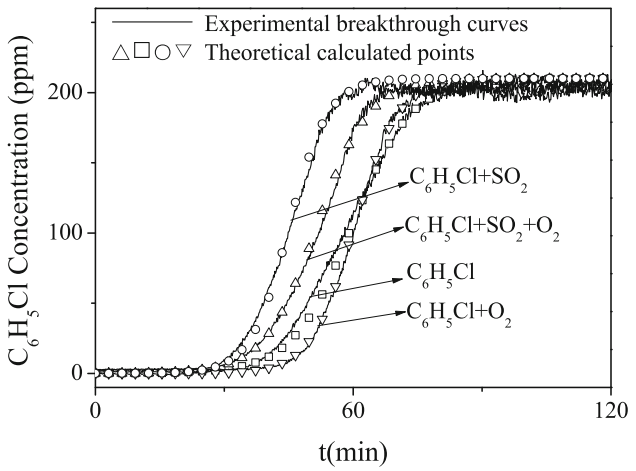

Fig. 5 Experimental and theoretical breakthrough curves for chlorobenzene (adsorption conditions: 200 ± 10 ppm chlorobenzene, 1000 ppm SO_2, 5 % O_2, N_2, 120 °C)

Table 4 Parameters for the Yoon-Nelson model for chlorobenzene adsorption

Gas composition	τ (min)	k'	C_6H_6Cl amount (mg/g)[a]	R^2
C_6H_5Cl	73.56	0.1456	65.17	0.9896
$C_6H_5Cl + SO_2$	58.98	0.2218	53.02	0.9867
$C_6H_5Cl + SO_2 + O_2$	65.40	0.1657	60.21	0.9942
$C_6H_5Cl + O_2$	74.18	0.1981	66.08	0.9962

[a] The chlorobenzene adsorption amounts were calculated based on Eq. (1)

In the presence of SO_2, the chlorobenzene breakthrough time is shortened by almost 15 min, so SO_2 seriously restricts chlorobenzene adsorption. The molecular polarity of SO_2 is 5.33×10^{-30} C·m, larger than 1.6×10^{-30} C·m of chlorobenzene, so SO_2 is more easily absorbed by the polar adsorption sites on the carbon. Moreover, the molecular diameter of SO_2 is 0.35 nm (Lide 1974), smaller than 0.77 nm of chlorobenzene, so SO_2 molecular diffusion is much faster than that of chlorobenzene and the SO_2 occupies the adsorption sites before the chlorobenzene. Therefore, SO_2 reduces the adsorption amount by 18.6 % for chlorobenzene, which shortens the time for the chlorobenzene adsorption to reach saturation.

In the presence of both SO_2 and O_2, the chlorobenzene adsorption amount was increased 10.8 % more than the simultaneous adsorption of SO_2 and chlorobenzene, but is 11.0 % less than for only chlorobenzene adsorption. The promotion effect of O_2 on the chlorobenzene adsorption is then relatively larger in the presence of SO_2.

The TPD-MS method was used to investigate the desorption characteristics of chlorobenzene and SO_2, with the results shown in Fig. 6. The initial decomposition temperature for chlorobenzene is 380 K, lower than 500 K for SO_2, and the turning temperature for the peak desorption concentration of chlorobenzene is 540 K, lower than 610 K for SO_2. The decomposition and turning temperatures are independent of the gas compositions; therefore, the SO_2 is much more stably adsorbed than chlorobenzene. Compared with previous TPD results (Shafeeyan et al. 2010; Rubel and Stencel 1997), most chlorobenzene is weakly physically adsorbed or combines with the carbon surface; while SO_2 is chemically adsorbed on carbon with almost all of the SO_2 oxidized by the activated carbon.

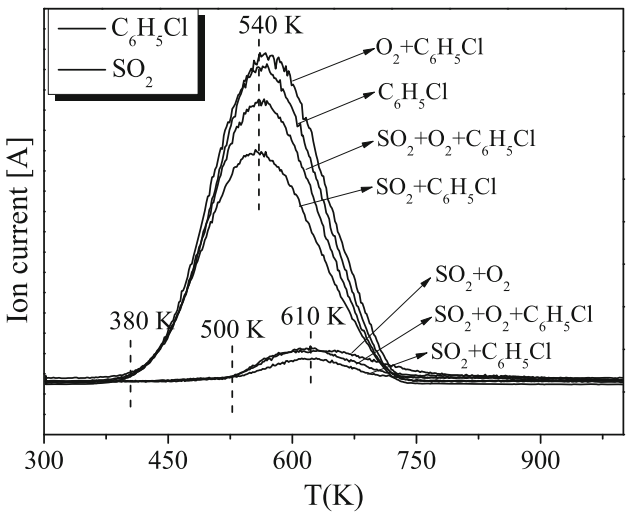

Fig. 6 TPD-MS profiles for chlorobenzene and SO_2

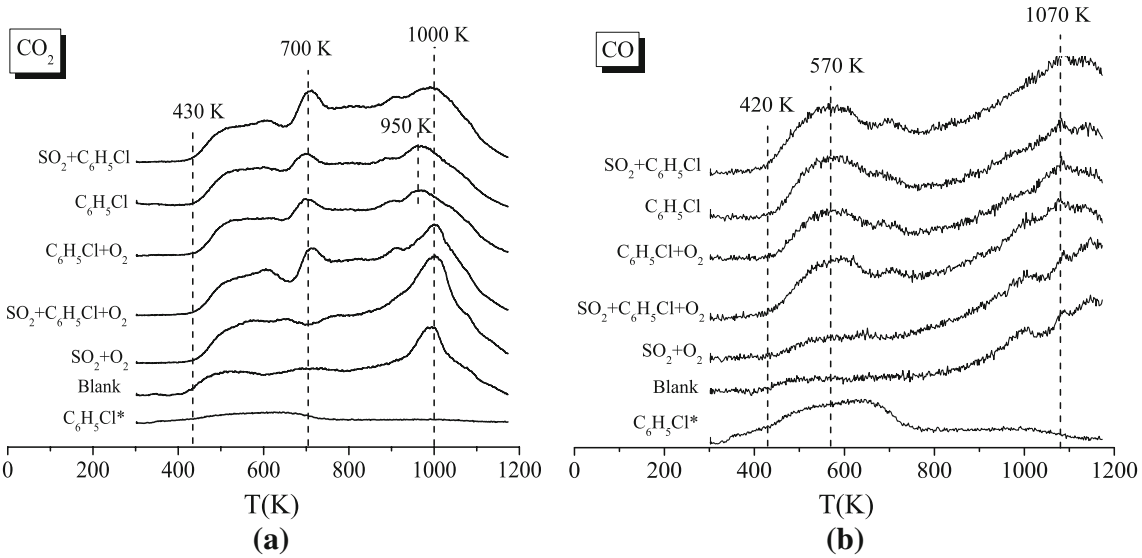

Fig. 7 TPD-MS profiles for CO_2 and CO (C_6H_5Cl* is the adsorbed chlorobenzene on the activated carbon treated at 1000 °C)

As the temperature increases, surface oxygen groups on the carbon decompose to release CO_2 at lower temperatures and predominantly CO at higher temperatures. The CO_2 is mainly from the decompositions of carboxyl and lactone groups, while the decomposition of carbonyl, quinone, phenol and ether groups produces CO (Shafeeyan et al. 2010). To further understand the interactions of the adsorbate with the carbon surface, the TPD-MS profiles for CO_2 and CO from the carbon decomposition are compared in Fig. 7. The activated carbon after adsorption in various atmospheres is desorbed in nitrogen, with the original activated carbon without any adsorbate desorbed as blank.

As shown in Fig. 7a, four desorption profiles for the chlorobenzene adsorption products were observed the CO_2 peak at 700 K. Two desorption profiles for the simultaneous adsorption of $SO_2 + O_2$ with or without chlorobenzene adsorption products were observed the CO_2 peak at 1000 K, with desorption profile of the blank sample giving a CO_2 peak at 1000 K. Figure 7b shows four desorption profiles for the chlorobenzene adsorption products were observed the CO peak at 570 and 1070 K, while the blank sample and the desorption product after the adsorption of $SO_2 + O_2$ did not give CO peaks.

As shown in Fig. 7a, b, the desorption profiles for the blank sample and the $SO_2 + O_2$ adsorption products shows no obvious changes in the surface groups except for small increase of the CO_2 desorption peak at 1000 K. Lactone groups decompose into CO_2 at 1000 K while carboxylic groups decompose into CO_2 at 673 K (Figueiredo and Pereira 2010). This indicates that some lactone groups are formed from the SO_2 oxidation in the presence of O_2, especially with the binary adsorption of SO_2 and chlorobenzene with and without O_2. The desorption temperature range of the CO peak at 570 K happens to correspond to that for chlorobenzene, so the peak at 570 K may be from the desorption of adsorbed chlorobenzene or the changed functional groups on the carbon after adsorption. To clarity the cause, the activated carbon was heated at 1000 °C for 1 h to remove the oxygen functional groups and then used in the TPD-MS test for chlorobenzene adsorption and desorption. The C_6H_5Cl* lines in Fig. 7 demonstrate that the peak at 570 K is caused by the desorption of adsorbed chlorobenzene.

The changes in the desorption of CO_2 and CO after chlorobenzene adsorption shows that the chlorobenzene could attach to the functional groups that released the CO_2 peak at 1000 K and the CO peak above 1070 K and these groups could have produced other functional groups for the CO_2 peak at 700 K after the chlorobenzene desorption. Thus, the lactone and quinone groups on the carbon tend to combine with chlorobenzene to form weak chemisorbed chlorobenzene, with the original groups transformed to carboxylic groups after the decomposition of the chemisorbed chlorobenzene.

According to the electron donor–acceptor mechanism, the atomic chlorine on chlorobenzene tends to give an electron to the carbon atom, which is combined with electron-withdrawing groups such as lactone and quinone to form the weak chemisorbed chlorobenzene. Chlorobenzene is then released upon heating and the original groups were transformed to carboxylic groups which decomposed around 700 K.

4 Conclusions

SO_2 adsorption is affected by the physical and chemical properties of activated carbon, especially the basic functional groups. Chlorobenzene adsorption is mainly affected

by the physical structure of the carbon, and the microporosity volume determines the adsorption amount, with larger size pores increasing the adsorption rate. Little influence of the chemical properties on chlorobenzene adsorption was observed.

SO_2 depresses the chlorobenzene adsorption, but the inhibitive effect decreases in the presence of O_2. O_2 has little promotion effect for the individual chlorobenzene adsorption, while the promotion effect becomes larger in the presence of SO_2. The TPD-MS results showed that the initial decomposition temperature was 380 K for chlorobenzene and 500 K for SO_2. Thus, SO_2 is more stably adsorbed by the carbon than chlorobenzene. Lactone and quinone groups were likely to combine with the chlorobenzene based on the electron donor–acceptor mechanism, with the groups probably transformed to carboxylic groups after the release of the chlorobenzene.

Acknowledgments This work was supported by the State 863 projects (No. 2012AA062501) and the Project of the Natural Science Foundation of China (No. 21177129).

References

Agranovski, I.E., Moustafa, S., Braddock, R.D.: Performance of activated carbon loaded fibrous filters on simultaneous removal of particulate and gaseous pollutants. Environ. Technol. **26**, 757–766 (2005)

Ahnert, F., Heschel, W.: Multicomponent adsorption of butane, NO_2 and SO_2 on activated carbon. Adsorpt. Sci. Technol. **20**, 353–370 (2002)

Asnin, L.D., Davankov, V.A., Pastukhov, A.V.: The adsorption of chlorobenzene on a carbon adsorbent obtained by the pyrolysis of hypercrosslinked polystyrene. Russ. J. Phys. Chem. A **82**, 2313–2317 (2008)

Bangham, D.H., Burt, F.P.: The behaviour of gases in contact with glass surfaces. Proc. R. Soc. Lond. Ser. A-Contain. Pap. Math. Phys. Charac. **105**, 481–488 (1924)

Biniak, S., Szymański, G., Siedlewski, J., Świątkowski, A.: The characterization of activated carbons with oxygen and nitrogen surface groups. Carbon **35**, 1799–1810 (1997)

Chiang, Y.C., Chiang, P.C., Chang, E.E.: Effects of surface characteristics of activated carbons on VOC adsorption. J. Environ. Eng.-ASCE **127**, 54–62 (2001)

Figueiredo, J.L., Pereira, M.F.R.: The role of surface chemistry in catalysis with carbons. Catal. Today **150**, 2–7 (2010)

Fournel, L., Mocho, P., Brown, R., Le Cloirec, P.: Modeling breakthrough curves of volatile organic compounds on activated carbon fibers. Adsorpt.-J. Int. Adsorpt. Soc. **16**, 147–153 (2010)

Ghimbeu, C.M., Gadiou, R., Dentzer, J., Vidal, L., Vix-Guterl, C.: A TPD-MS study of the adsorption of ethanol/cyclohexane mixture on activated carbons. Adsorpt.-J. Int. Adsorpt. Soc. **17**, 227–233 (2011)

Gironi, F., Piemonte, V.: VOCs removal from dilute vapour streams by adsorption onto activated carbon. Chem. Eng. J. **172**, 671–677 (2011)

Goworek, J., Swiatkowski, A., Biniak, S.: Characterization of modified active carbons by adsorption of pure water and benzene vapors and ternary liquid mixture benzene plus diethyl ketone plus n-heptane. Langmuir **13**, 1225–1228 (1997)

Huang, C.C., Lin, Y.C., Lu, F.C.: Dynamic adsorption of organic solvent vapors onto a packed bed of activated carbon cloth. Sep. Sci. Technol. **34**, 555–570 (1999)

Izquierdo, M.T., Rubio, B., Mayoral, C., Andrés, J.M.: Low cost coal-based carbons for combined SO_2 and NO removal from exhaust gas. Fuel **82**, 147–151 (2003)

Karatepe, N., Orbak, İ., Yavuz, R., Özyuğuran, A.: Sulfur dioxide adsorption by activated carbons having different textural and chemical properties. Fuel **87**, 3207–3215 (2008)

Karpowicz, F., Hearn, J., Wilkinson, M.C.: Dynamic adsorption of vapours by activated carbons and by polymer-derived adsorbents: 1. Adsorption at 0% RH. Adsorpt.-J. Int. Adsorpt. Soc. **6**, 337–347 (2000)

López, D., Buitrago, R., Sepúlveda-Escribano, A., Rodríguez-Reinoso, F., Mondragón, F.: Low temperature catalytic adsorption of SO_2 on activated carbon. J. Phys. Chem. C Nanomater Interfaces **112**, 15335 (2008)

Lide D.R. (ed.): CRC Handbook of Chemistry and Physics, vol. 55. CRC Press, Boca Reton, FL (1974)

Liu, Z.S.: Adsorption of SO_2 and NO from incineration flue gas onto activated carbon fibers. Waste Manage. **28**, 2329–2335 (2008)

Mastral, A.M., Garcia, T., Murillo, R., Callen, M.S., Lopez, J.M., Navarro, M.V.: Effects of CO_2 on the phenanthrene adsorption capacity of carbonaceous materials. Energy Fuels **16**, 510–516 (2002)

Montes-Morán, M.A., Suárez, D., Ménendez, J.A., Fuente, E.: On the nature of basic sites on carbon surfaces: an overview. Carbon **42**, 1219–1225 (2004)

Raymundo-Piñero, E., Cazorla-Amorós, D., de Lecea, C.S.M., Linares-Solano, A.: Factors controlling the SO_2 removal by porous carbons: relevance of the SO_2 oxidation step. Carbon **38**, 335–344 (2000)

Raymundo-Piñero, E., Cazorla-Amorós, D., Linares-Solano, A.: Temperature programmed desorption study on the mechanism of SO_2 oxidation by activated carbon and activated carbon fibres. Carbon **39**, 231–242 (2001)

Rubel, A.M., Stencel, J.M.: The effect of low-concentration SO_2 on the adsorption of NO from gas over activated carbon. Fuel **76**, 521–526 (1997)

Santoro, D., de Jong, V., Louw, R.: Hydrodehalogenation of chlorobenzene on activated carbon and activated carbon supported catalysts. Chemosphere **50**, 1255–1260 (2003)

Shafeeyan, M.S., Daud, W., Houshmand, A., Shamiri, A.: A review on surface modification of activated carbon for carbon dioxide adsorption. J. Anal. Appl. Pyrolysis **89**, 143–151 (2010)

Suzuki, M.: Adsorption Engineering. Kodansha-Elsevier, Amsterdam (1990)

Vanosdell, D.W., Owen, M.K., Jaffe, L.B., Sparks, L.E.: VOC removal at low contaminant concentrations using granular activated carbon. J. Air Waste Manage. Assoc. **46**, 883–890 (1996)

Zhang, P., Wanko, H., Ulrich, J.: Adsorption of SO_2 on activated carbon for low gas concentrations. Chem. Eng. Technol. **30**, 635–641 (2007)